Biophysical Chemistry 144 (2009) 27–37

Contents lists available at ScienceDirect

Biophysical Chemistry

journal homepage: http://www.elsevier.com/locate/biophyschem

Poly-L-lysines and poly-L-arginines induce leakage of negatively charged phospholipid vesicles and translocate through the lipid bilayer upon electrostatic binding to the membrane

Marcel Reuter [a,1], Christian Schwieger [a,2], Annette Meister [a], Göran Karlsson [b], Alfred Blume [a,*]

[a] Institute of Chemistry, Martin-Luther-University Halle-Wittenberg, Muehlpforte 1, 06108 Halle, Germany
[b] Department of Physical and Analytical Chemistry, Uppsala University, Box 579, 75123 Uppsala, Sweden

ARTICLE INFO

Article history:
Received 4 March 2009
Received in revised form 29 May 2009
Accepted 2 June 2009
Available online 10 June 2009

Keywords:
Phospholipid membranes
Cationic polypeptides
Peptide–lipid interactions
Dye-release assay

ABSTRACT

Poly-L-lysines (PLL) and poly-L-arginines (PLA) of different polymer chain lengths interact strongly with negatively charged phospholipid vesicles mainly due to their different electrical charges. 1-Palmitoyl-2-oleoyl-*sn*-glycero-3-phosphoglycerol (POPG), 1,2-dipalmitoyl-*sn*-glycero-3-phosphoglycerol (DPPG) and their mixtures (1/1 mol/mol) with the respective phosphatidylcholines of equivalent chain length were chosen as model membrane systems that form at room temperature either the fluid L_α or the gel phase L_β lipid bilayer membranes, respectively. Leakage experiments revealed that the fluid POPG membranes are more perturbed compared to the gel phase DPPG membranes upon peptide binding. Furthermore, it was found that pure PG membranes are more prone to release the vesicle contents as a result of pore formation than the lipid mixtures POPG/POPC and DPPG/DPPC. For the longer polymers (≥44 amino acids) maximal dye-release was observed when the molar ratio of the concentrations of amino acid residues to charged lipid molecules reached a value of $R_P = 0.5$, i.e. when the outer membrane layer was theoretically entirely covered by the polymer. At ratios lower or higher than 0.5 leakage dropped significantly. Furthermore, PLL and PLA insertions and/or translocations through lipid membranes were analyzed by using FITC-labeled polymers by monitoring their fluorescence intensity upon membrane binding. Short PLL molecules and PLA molecules of all lengths seemed to translocate through both fluid and gel phase lipid bilayers. Comparison of the PLL and PLA fluorescence assay results showed that PLA interacts stronger with phospholipid membranes compared to PLL. Isothermal titration calorimetry (ITC) measurements were performed to give further insight into these mechanisms and to support the findings obtained by fluorescence assays. Cryo-transmission electron microscopy (cryo-TEM) was used to visualize changes in the vesicles' morphology after addition of the polypeptides.

1. Introduction

Since the 1970s many publications on lipid interactions with cationic polypeptides have appeared [1–4]. The major interest in these studies arises from cell biology [5] and from drug delivery investigations [6]. In pharmaceutical applications poly-L-lysines (PLLs) and poly-L-arginines (PLAs) serve as model compounds for the distribution of biologically active substances in organisms and different tissues [7]. It was shown that PLLs and PLAs in high concentrations have anticarcinogenic properties [8]. Cationic polypeptides also serve as models for cell toxic and antimicrobial peptides [9,10]. A particularly important function of arginine-rich peptides is their assistance of the internalization of the HI-virus into cells via Tat protein interactions [11–14].

Binding of these cationic polypeptides to negatively charged phospholipid membranes leads to the formation of large aggregates [15,16]. Peptide binding results in a perturbation of the phospholipid membrane, which is an important step for processes like vesicle leakage and in some cases subsequent lysis, peptide translocation, membrane and vesicle fusion and lipid phase transformation.

Pore formation and vesicle lysis can be analyzed with a dye-release assay based on liposomes which contain a high amount of a self-quenching fluorescent dye in the inner volume. Dequenching takes place when the dye is released into the solution due to membrane rupture. With this method it was shown that PLLs cause pore formation in 1,2-dipalmitoyl-*sn*-glycero-3-phosphoglycerol/1,2-dipalmitoyl-*sn*-glycero-3-phosphatidylcholine DPPG/DPPC membranes on a timescale of one week [16]. Using a similar approach

* Corresponding author.
E-mail address: alfred.blume@chemie.uni-halle.de (A. Blume).
[1] Present address: School of Chemistry, The University of Edinburgh, West Mains Road, EH9 3JJ Edinburgh, Scotland, United Kingdom.
[2] Present address: Institute Nationale de la Recherche Agronomique (INRA) Unité Biopolymers, Interaction, Assemblage, BP 71627, 44316 Nantes Cedex 3, France.

0301-4622/$ – see front matter © 2009 Elsevier B.V. All rights reserved.
doi:10.1016/j.bpc.2009.06.002

Young and Kauss [17] found that PLLs increase cell membrane permeability with increasing PLL length.

Endocytosis is an important biological mechanism involved in the uptake of macromolecules and particles into cells that is relevant in medical applications. PLL, PLA [18] and their shorter homologues oligo–arginine [14] and oligo–lysine assist this process according to their abilities of charge shielding and aggregation when binding to negatively charged membranes and/or drug molecules [19]. This effect plays a role in the cellular uptake of viruses [11,12] and oligonucleotides [6]. Also, PLL and PLA are able to translocate through lipid membranes without being complexed as shown by Shibata et al. [20] and Sakai & Matile [4].

Fuchs & Raines [13,18] analyzed and explained the key steps of the process of peptide translocation through cell membranes: PLA first binds to heparan sulphates exposed on the outer cell membrane which is followed by endocytotic uptake. PLA is then released into the cytoplasm after degradation of the binding component with subsequent leakage from the transferring vesicles.

Membrane binding and destabilization are also important in membrane and vesicle fusion. Bondeson & Sundler [21] pointed out that the oligo- and polymers of the three naturally occurring basic amino acids and ornithine induce membrane fusion of negatively charged vesicles while acidification of the lipid suspension (pH 5 to 6) acts as a trigger. Similar studies were carried out by Walter et al. [22] and Gad et al. [2] who found that cross linking of two negatively charged vesicles is an important step in membrane fusion. Gad et al. proposed that longer polymers have a stronger tendency to induce the fusion process than shorter ones at the same (amino acid residue) concentration whereas Walter et al. challenged this proposal. An excellent review of polymer and cation induced membrane fusion was published by Arnold [23].

PLL and PLA interactions with phospholipid membranes were studied using a wide range of different methods: X-ray analyses showed that phospholipid suspensions in high concentrations form stable multilayers when the negative charge of DPPG molecules (in the gel phase) is neutralized upon PLL binding (>44 amino acid residues) which intercalate between two bilayers as helices [24]. Secondary structure transitions of PLL after binding to gel phase membranes from coil to alpha-helix or beta-sheet were investigated using FT-IR [25] and calorimetric methods, such as DSC and ITC. Binding of PLL and PLA to membranes leads to changes in the lipid main transition temperature and in the order of the lipid chains [25]. ITC was shown to be ideally suited to follow peptide adsorption on membrane surfaces [26,27]. Atomic force microscopy [28], dynamic light scattering [15,27], and electron microscopy [2] revealed in particular aggregation effects and allowed their quantitative evaluation. Zeta potential measurements were performed to evaluate the surface charge of vesicles and the changes after peptide binding [15].

Theoretical calculations showed that the dominating contribution to the binding affinity is the release of counter-ions from the surface when the polymer is bound [29]. It was found that the charge densities of both macromolecular (polypeptide) and supramolecular (lipid membrane) entity have to be of the same order to allow efficient adsorption [30]. Despite numerous studies on the binding of polyelectrolytes to lipid membranes a number of open questions remain, particularly about the importance of non-electrostatic contributions to the binding affinity. Another question that needs to be addressed is the efficiency of PLL and PLA to induce vesicle leakage as a function of polypeptide chain length. In this publication we focus on the interactions of PLL and PLA of different lengths to phospholipid membranes composed of either phosphatidylglycerols (PG) molecules or 1/1 mol/mol mixtures of PG and phosphatidylcholines (PC) in both the fluid and the gel phase. Leakage behavior of phospholipid vesicles induced by peptide binding is addressed in the same way as the translocation studies of PLL and PLA through lipid membranes. An intensive kinetic study of these processes is presented aiming at a comparison and deconvolution of these two effects. ITC studies were performed to complement the leakage and translocation investigations. Peptide induced changes in the morphology of the phospholipid vesicles were investigated using cryo-TEM.

2. Materials and methods

2.1. Peptides and FITC labeling procedure

Poly-L-lysines (hydrobromide salts) with average molecular weights between 1000 and 5000, 4000 and 15,000, 15,000 and 30,000, 30,000 and 70,000, 70,000 and 150,000 and 150,000 and 300,000 were purchased from Sigma-Aldrich (Steinheim, Germany). FITC-labeled PLLs (hydrobromide salts, the labeling ratio is 1 dye molecule/200 lysine residues) of a molecular weight between 15,000 and 30,000 and 30,000 and 70,000 and PLAs (hydrochloride salts) of 5000 to 15,000, 15,000 to 70,000 and higher than 70,000 were also obtained from Sigma. The average molecular weight which differed slightly from batch to batch was determined by the supplier using viscosity measurements. Throughout this article the average number of amino acid residues in one peptide molecule is given.

FITC-PLAs were synthesized according to a method described by Fülöp et al. [31]. 10 mg (0.0512 mmol) PLA and 0.0997 mg FITC (2.56×10^{-4} mmol, from a stock solution, from Sigma-Aldrich) were dissolved in 0.5 ml DMSO (analytical grade, Sigma-Aldrich GmbH, Deisenhofen, Germany) under nitrogen to obtain a labeling ratio of 0.005 mol FITC/1 mol arginine residues. This mixture was stirred in the dark for three days at room temperature. The reaction was followed using thin layer chromatography (TLC) with a 50/50 v/v solvent mixture of DMSO and distilled water. R_F values for FITC and FITC-PLA were 1 and 0, respectively. DMSO was removed by freeze-drying. For purification the raw product was dissolved in distilled water and was dialyzed against 100 ml distilled water using a 3.5 kDa cut-off membrane (SERVA Spectra/Por, Heidelberg, Germany) and a micro dialysis capsule (Carl Roth GmbH + Co. KG, Karlsruhe, Germany). The distilled water was replaced every 12 h. Purity checks were performed using TLC. Eventually, the purified product was obtained by freeze-drying. The yields were between 70 and 80% for both FITC-PLA samples. 1 and 10 mM stock solutions of peptides in 100 mM NaCl solution were prepared, stored in the refrigerator at 4 °C, and used for a maximum of up to four weeks.

2.2. Preparation of vesicles for dye-release, translocation and ITC assays

All lipids (POPG, POPC, DPPG, and DPPC) were purchased from Genzyme (Liestal, Switzerland) and used without further purification. Phospholipid vesicles with entrapped calcein (disodium salt) (Fluka Chemie GmbH, Buchs, Switzerland) for dye-release assays were prepared according to New [32]. 267.53 mg (0.4 mmol) calcein were dissolved in 5 ml deionized water (SG Wasseraufbereitung und Regenerierstation GmbH, Hamburg-Barsbüttel, Germany) yielding a 80 mM dye solution. 15.76 mg (0.02 mmol) POPG were suspended in 4 ml 80 mM calcein solution by heating to 50 °C and vortexing (two to three times) giving a 5 mM POPG (dye) suspension. 1 ml aliquots of this suspension were extruded 15 times using an Avestin extruder (Ottawa, Canada) through two polycarbonate membranes with a pore size of 100 nm (Avanti Polar Lipids, Inc., Alabaster, AL, USA) to produce large unilamellar vesicles (LUVs). The extrusion temperature was maintained 10 K above the phase transition temperature (T_m (POPG) = 4 °C). The external calcein dye was removed by centrifugation of the suspension through a column filled with Sephadex G-75 gel (Pharmacia, Uppsala, Sweden). Each suspension was centrifuged twice at 3000 rpm for 3 min using a fresh column for each centrifugation step (Biofuge 17RS, Heraeus Sepatech GmbH, Osterode, Germany). Directly after the centrifugation the eluted lipid suspensions were mixed with an equivalent volume of 100 mM NaCl solution

to prevent an osmotic gradient which could lead to vesicle rupture. Each vesicle suspension was stored at 4 °C and used for up to 4 days. The vesicle size was controlled by DLS and was found to be in the diameter range of 100 to 120 nm. DLS measurements were carried out using an ALV-NIBS/HPPS (ALV-Laser Vertriebsgesellschaft mbH, Langen, Germany). Vesicles were checked for dye-release every day revealing no leakage when stored at 4 °C.

Lipid suspensions for ITC and experiments with FITC-labeled peptides were prepared in a 100 mM NaCl solution and were extruded and characterized as described before. Vesicles containing different lipids, i.e. PG and PC, were prepared from 5 mM standard solutions in chloroform and a small amount of methanol (HPLC grade solvents, Carl Roth GmbH) to ensure homogenous lipid distribution in the vesicles. Equivalent amounts of stock solutions were mixed to obtain 1/1 molar ratios of PG and PC. The solvent was removed by heating the solution to 40 °C and subjecting it to a dry nitrogen stream until all solvent evaporated. The lipid film was dried for 12 h under vacuum and was finally suspended in 100 mM NaCl. The lipid suspension was then extruded and checked as described before.

2.3. Phosphate determination assay

The lipid content of the used vesicle suspensions was determined based on the phosphate determination assays by Chen et al. and Fiske & Subbarow [33,34]. The content of each sample was determined three times.

2.4. Fluorescence assays

Fluorescence measurements were carried out using a FluoroMax-2 fluorescence spectrometer (Instruments S.A. GmbH, Grasbrunn, Germany). Excitation and emission wavelengths for calcein and FITC are similar with 490 and 520 nm, respectively. Dye-release assays were performed at 22 °C and experiments with FITC-labeled peptides at 20 °C. All kinetic experiments in aqueous suspensions were done in PS cuvettes (Sarstedt AG & Co., Nümbrecht, Germany). Spectra acquisition in organic solvents was performed in quartz cuvettes.

For the dye-release experiments a peptide solution, containing either PLL or PLA, with a salinity of 100 mM was stirred continuously in the cuvette inside the spectrometer while detecting the fluorescence signal. After an equilibration time of 30 s a well-defined amount of calcein charged phospholipid vesicles was added to reach a lipid concentration of 100 µM. Dye-release from the vesicles was followed over a time period of 690 s. Then, 100 µl of a 5% Triton X-100 solution (Sigma-Aldrich) was added to determine the value of maximal dye-release. During a sequence of experiments the peptide concentration was varied but the lipid concentration was kept constant.

Experiments with FITC-labeled polymers were carried out similarly to the dye-release experiments. Peptide solutions in a cuvette were stirred continually for a minute and then a well-defined amount of lipid suspension was added to reach a final lipid concentration of 100 µM. FITC is an analogous dye to calcein which changes its quantum yield depending on the chemical environment. For the three different solvents water, DMSO and chloroform the relative quantum yields are 0.9, 0.8 and $5*10^{-3}$, respectively. When FITC-labeled PLL or PLA bind to the lipid membranes the fluorescence intensity will decrease strongly. If every FITC moiety would insert into the lipid membrane, the normalized FITC-fluorescence intensity would drop to 0.01.

2.5. Isothermal titration calorimetry (ITC)

ITC measurements were performed using a VP-ITC (MicroCal Inc., Northhampton, MA, USA). The cell with a volume of 1.4 ml contained either a 2 or 4 mM lipid suspension (average vesicle diameter 110 nm) which was degassed directly before the experiment. 271 µl of a 20 mM peptide solution was injected with a stirred syringe (stirring speed 270 rpm) with the following sequence (in brackets the delay time after an injection is given): 1×1 µl (300 s) and 27×10 µl (900 s). Processing of the results was done with the Origin software for ITC data (provided by MicroCal Inc.). The enthalpy value of the first injection was omitted due to experimental errors.

2.6. Cryo-TEM

The electron microscopy investigations were performed with a Zeiss 902A instrument, operating at 80 kV. Specimens were prepared by a blotting procedure, performed in a chamber with controlled temperature and humidity. A drop of the sample solution (1 mg ml^{-1}) was placed onto an EM grid coated with a perforated polymer film. Excess solution was then removed with a filter paper, leaving a thin film of the solution spanning the holes of the polymer film on the EM grid. Vitrification of the thin film was achieved by rapid plunging of the grid into liquid ethane held just above its freezing point. The vitrified specimen was kept below 108 K during both, transfer to the microscope and investigation.

POPG-polypeptide samples were prepared by adding the desired quantity of 1 mM polypeptide solution to 40 µl of an extruded 5 mM POPG suspension and completion to 2 ml with water. For all samples the concentration of NaCl was adjusted to 100 mM.

3. Results

3.1. Dye-release of phospholipid vesicles upon PLL and PLA binding

The dye-release experiments were performed as described above. In the figure legends the ratio of the overall concentration of amino acid residues (lysines or arginines, respectively) to the concentration of charged lipid molecules, i.e. PG molecules, is given. This molar ratio is denoted R_P. From previous experiments it is well-known that the fluorescence intensity is directly proportional to the calcein concentration in the concentration range from 0.01 to 10 µM. A further increase in calcein concentration to 100 and 1000 µM leads to a 30 and 10,000 fold drop in fluorescence intensity, respectively, due to a self-quenching of the dye. The calcein concentrations have been chosen to obtain a maximum fluorescence intensity difference during the leakage experiments.

3.2. Dye-release from POPG and DPPG

Leakage experiments were performed with POPG, DPPG, POPG/POPC and DPPG/DPPC vesicles (1/1 mol/mol) at room temperature in order to evaluate the influences of both the lipid phase state (either L_α or L_β) and the charge density on vesicle lysis and the occurrence of membrane defects, induced by PLLs and PLAs of different polymer lengths. Dye-release kinetic curves from POPG and DPPG vesicles induced by PLL 44 are shown in Fig. 1a and b, respectively. At low and high R_P values of 0.13 and 1.28, respectively, PLL 44 does not induce any significant dye-release from POPG vesicles. At R_P values of 0.26, 0.38 and 0.52 a continuously increasing leakage is observed. The first of the fluorescence intensity curves has an exponential shape which transforms then into a rather sigmoidal curve form for higher R_P values. At an R_P of 0.64 the intensity increase has a sigmoidal form and the kinetics of dye-release is decreased so that maximally expected dye-release is not reached within the chosen observation time.

In the case of DPPG vesicles the dye released from vesicles due to PLL 44 interactions reaches a maximum of 41% at an R_P of 1.19. The R_P regime where leakage occurs (from 0.36 to 1.19) is larger than in the case of POPG. The curve shapes are either slightly sigmoidal ($R_P = 0.64$) or exponential ($R_P = 1.28$). At low and high R_P values of 0.12 and 3.57 the leakage reaches a minimum (<5%).

The kinetic curves for dye-release from POPG vesicles that are induced by PLA 69 are shown in Fig. 1c. At R_P values lower than 0.13

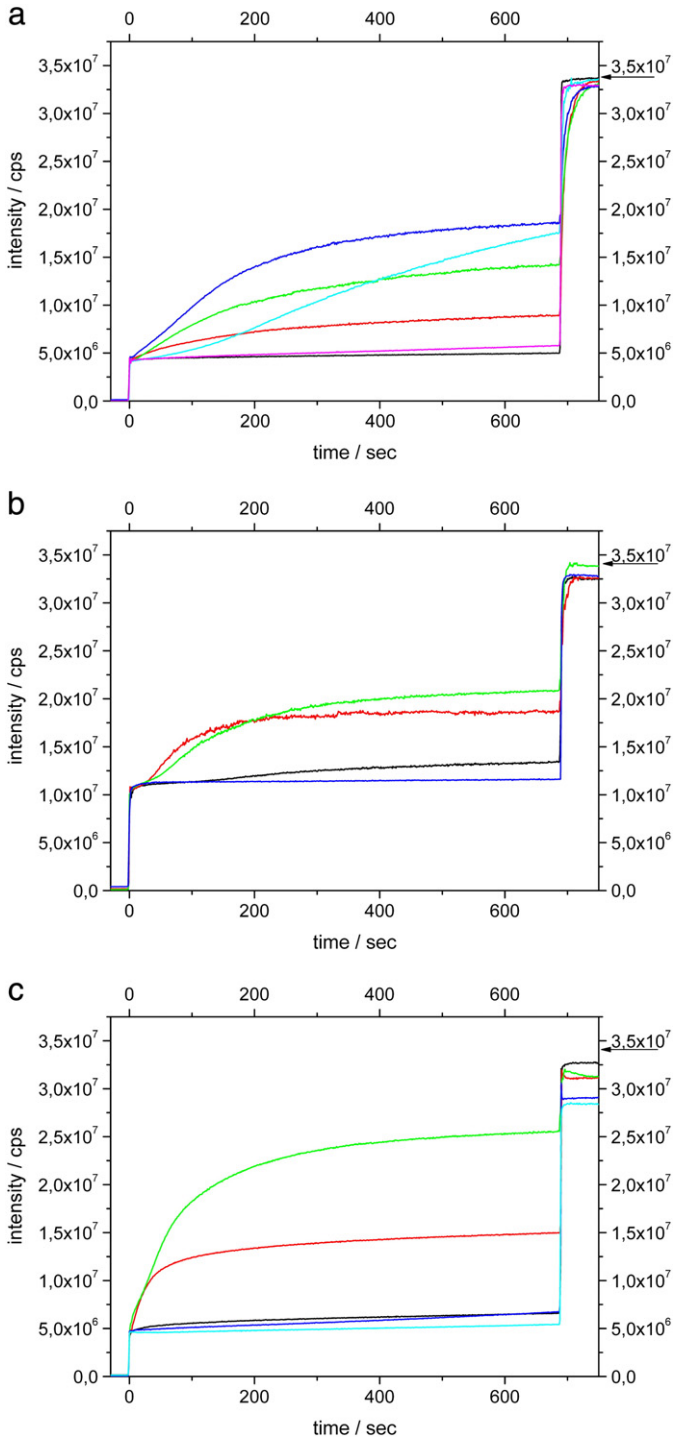

Fig. 1a: Dye-release kinetic curves of PLL 44 interaction with POPG vesicles. In different experiments the PLL concentration was varied, so that R_P values of 0.13 (-), 0.26 (-), 0.38 (-), 0.51 (-), 0.64 (-) and 1.28 (-) were obtained. After an equilibration time of 30 s a well-defined amount of calcein-carrying vesicles was added (time point of 0 s in the graph) which was kept constant at 80 μM in all experiments. The reaction temperature was 22 to 23 °C. Fig. 1b: Dye-release kinetic curves of PLL 44 interaction with DPPG vesicles. In different experiments the PLL concentration was varied, so that R_P values of 0.12 (-), 0.6 (-), 1.19 (-), and 3.57 (-) were obtained. (After an equilibration time of 30 s a well-defined amount of calcein-carrying vesicles was added (time point of 0 s in the graph) which was kept constant at 85 μM in all experiments.) The reaction temperature was 22 to 23 °C. Fig. 1c: Dye-release kinetic curves of PLA 69 interaction with POPG vesicles. In different experiments the PLA concentration was varied, so that R_P values of 0.13 (-), 0.38 (-), 0.64 (-), 1.28 (-) and 3.85 (-) were obtained. After an equilibration time of 30 s a well-defined amount of calcein-carrying vesicles was added (time point of 0 s in the graph) which was kept constant at 75 μM in all experiments. The reaction temperature was 22 to 23 °C.

and higher than 1.28 less than 10% of the entrapped dye molecules are released into the solution. At intermediate R_P values of 0.38 and 0.64 a leakage of 33 and 66% are observed, respectively. Both curves appear to be bi-exponential indicating two processes that originate possibly from membrane disordering and pore formation. For an R_P value of 0.38 the time constants t_1 and t_2 are approximately 25 s and 300 s,

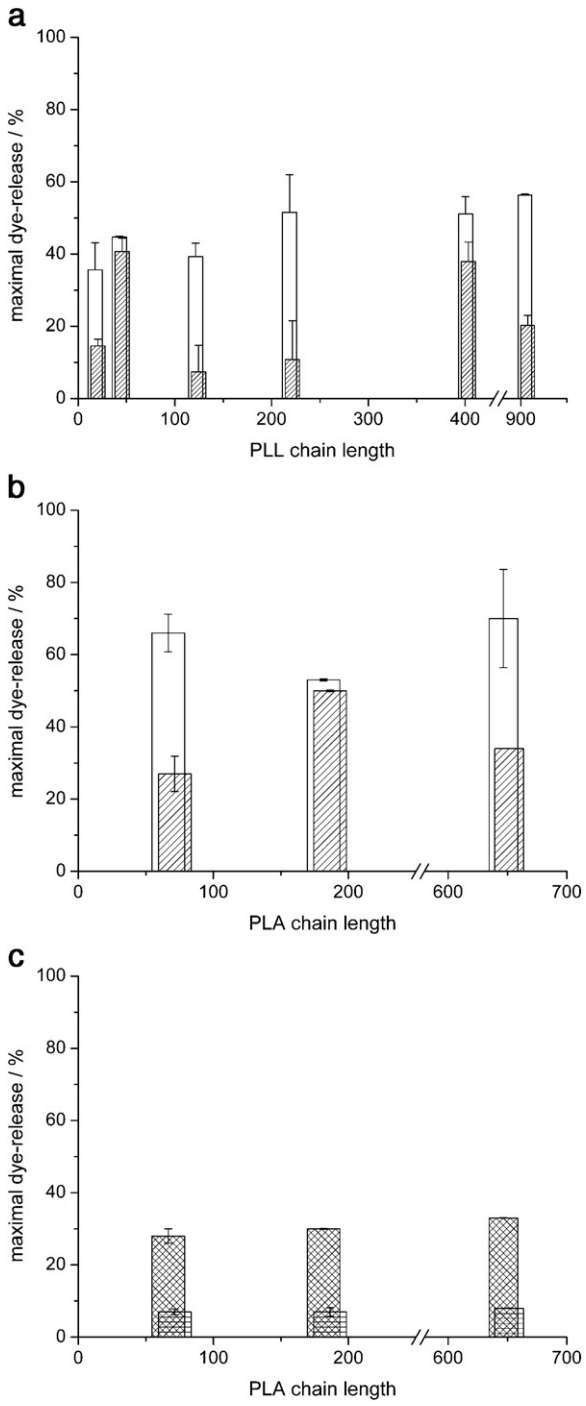

Fig. 2. Maximal dye-release from POPG and DPPG and mixed vesicles induced by PLLs and PLAs. a): Maximal dye-release from POPG (empty bar) and DPPG (diagonally dashed bar) vesicles induced by PLLs of the average lengths 19, 44, 123, 220, 402 and 906. b): Maximal dye-release from POPG (empty bar) and DPPG (diagonally dashed bar) vesicles induced by PLAs of the average lengths 69, 184 and 649. c): Maximal dye-release from POPG/POPC (1/1 mol/mol) (patterned bar) and DPPG/DPPC (1/1 mol/mol) (horizontally dashed bar) vesicles induced by PLAs of the average lengths 69, 184 and 649.

respectively. At an R_P of 0.64 these time constants t_1 and t_2 are similar with 63 and 278 s, respectively.

3.3. Comparison of maximal dye-release of POPG and DPPG vesicles depending on PLLs and PLAs of different chain length

Dye-release curves were monitored for PLLs with different lengths interacting with pure POPG and DPPG vesicles and for PLAs with different lengths binding to pure lipid vesicles and mixed vesicles of PG and PC. The maximal relative dye-release in % was calculated according to the formula: dye-release $(\%) = 100 \cdot (I_{690\ s} - I_{0\ s}) / (c_{dil} * I_{720\ s} - I_{0\ s})$ where the intensity value at 720 s was taken after addition of Triton X-100, thus the introduction of a dilution factor c_{dil} (2.1/2). The maximum values for each PLL and PLA length are shown in Fig. 2a–c. The leakage was highest for lipids in the fluid L_α phase and decreased for lipids in the gel phase L_β. The PG/PC lipid mixtures showed a further decrease in dye-release. The amount of dye released from POPG vesicles by PLLs of lengths from 19 to 906 varied between 36 and 56%. The dye-release values increased with increasing PLL length except for PLL 44. For DPPG gel state vesicles the maximal dye-release varied more strongly with differing polymer length. No clear trend could be observed, except a somewhat higher leakage for the shorter PLLs. For all longer PLLs ($\geq$44) a maximal dye-release is reached at a R_P value of 0.5 ± 0.1. PLL 19 causes an increasing vesicle leakage until it reaches an R_P value of 4 with a maximum leakage rate of 36% (Fig. 3a–b).

PLA induced maximum leakage for POPG vesicles ranging from 60 to 80% with a minimum for PLA 184 which has an intermediate chain length. In the case of gel state DPPG vesicles the dye-release was lower without significant trend. In the case of the fluid POPG/POPC and gel state DPPG/DPPC vesicles no significant differences between the different polymer lengths were observed. However, dye-release was generally lower than for the pure POPG or DPPG vesicles. All PLAs cause only little leakage ($\leq$10%) from POPG vesicles at R_P values either smaller than 0.13 or higher than 1.28. Maximal dye-release occurs at an R_P of 0.38 (for PLA 184) and 0.64 (for PLA 69 and 649) (Fig. 3c).

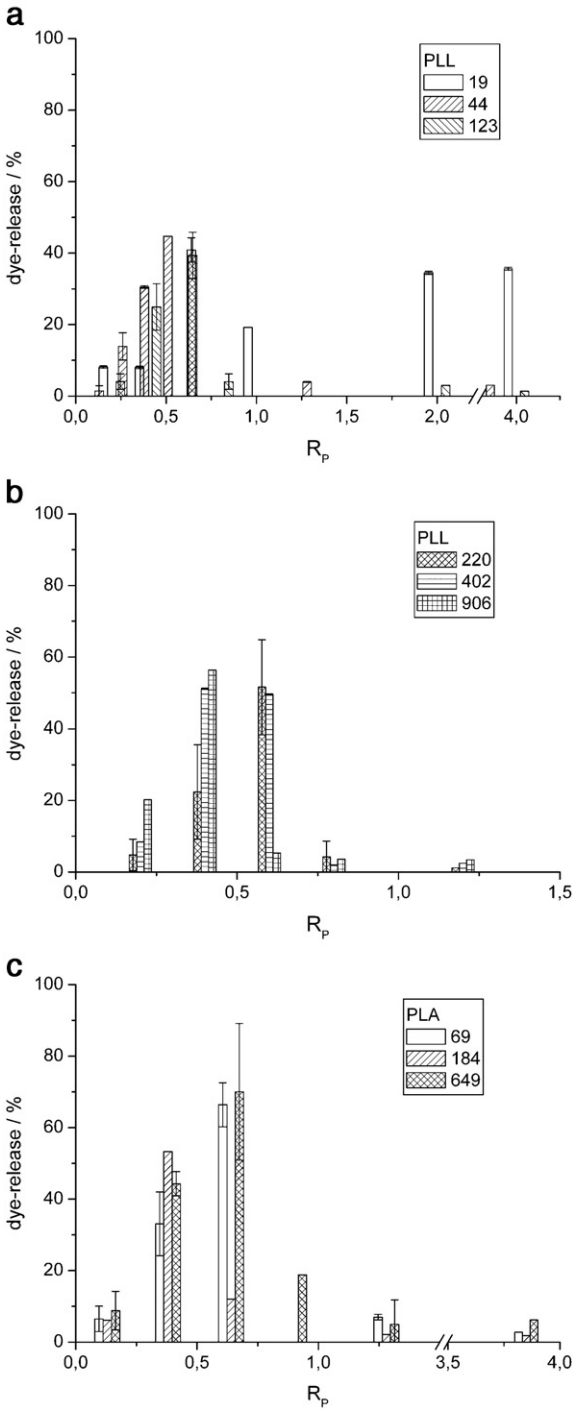

Fig. 3. POPG dye-release dependence on R_P (PLLs and PLAs). a): Dye-release from POPG vesicles as a function of R_P for PLLs 19, 44 and 123. b): Dye-release from POPG vesicles as a function of R_P for PLLs 220, 402 and 906. c): Dye-release from POPG vesicles as a function of R_P for PLAs 69, 184 and 649.

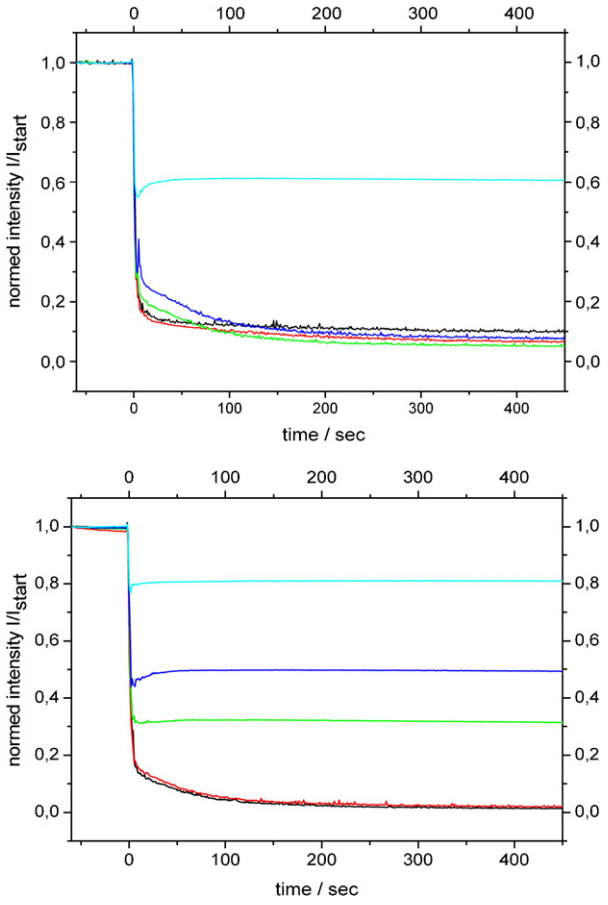

Fig. 4. FITC-PLL 106 (upper panel) and FITC-PLL 319 (lower panel) binding to DPPG vesicles. While varying the FITC-PLL concentration in different experiments, DPPG vesicles at a constant lipid concentration of 100 μM have been injected at a time point of 0 s and the binding of FITC-PLL was monitored (with time). R_P values are as follows: 0.4 (-), 0.5 (-), 0.8 (-), 1 (-) and 2 (-). The reaction temperature was 22 to 23 °C.

Table 1
Membrane binding of FITC-labeled PLLs and PLAs.

		Short	Long
POPG	PLL	0.06	0.49
	PLA	0.26	0.17
DPPG	PLL	0.07	0.49
	PLA	0.1	0.34
POPG/POPC	PLL	0.05	0.46
	PLA	0.21	0.39
DPPG/DPPC	PLL	0.09	0.63
	PLA	0.12	0.39

FITC-PLL (106 (short) and 319 (long)) and FITC-PLA (69 (short) and 649 (long)) binding to POPG–, DPPG–, POPG/POPC (1/1 mol/mol) and DPPG/DPPC (1/1 mol/mol) vesicles. In the table the normalized fluorescence intensity values after membrane binding for $R_P = 1$ at a time point of 840 s are shown.

3.4. Binding of FITC-labeled PLL 106 and 319 to DPPG membranes

Binding studies of FITC-labeled PLL 106 and 319 to DPPG membranes were performed to check whether the different PLLs are binding to negatively charged DPPG membranes. FITC-PLL 106 and FITC-PLL 319 solutions of different concentrations were chosen to match R_P values of 0.4, 0.5, 0.8, 1 and 2. When DPPG vesicles are injected into these peptide solutions (Fig. 4a–b) the first step of peptide binding to the phospholipid membranes occurs very fast. Depending on the actual peptide and the R_P value a second much slower process occurs on a time scale as observed in the dye-release experiments.

At an R_P value of 0.4 and 0.5 FITC-PLL 106 binds in two steps to the DPPG membrane: The first step is very fast and leads to a drop in the normalized fluorescence intensity to 0.15 whereas the second step requires 300 s and more until a constant fluorescence intensity value of 0.1 is reached. For the higher R_P values of 0.8 and 1 the first binding step shows a smaller drop in fluorescence intensity to 0.2 and 0.25. The second step is now characterized by a sigmoidal decay of the normalized fluorescence intensity which ends at a slightly lower value of 0.07 and 0.09. At an even higher R_P value of 2 the sudden drop in the fluorescence intensity occurs only to 0.55 and then increases again to a value of 0.6.

FITC-PLL 319 shows principally similar kinetic binding curves. However, there is a characteristic shift in the final normalized fluorescence intensities for the same R_P values compared to the experiments with FITC-PLL 106. Particularly for the R_P values of 0.4 and 0.5 the kinetic curves obtained with the two PLLs are very similar. After lipid injection, both curves show a fast drop in fluorescence intensity to 0.15 followed by a slow exponential decrease to a value of 0.05. For the R_P values 0.8, 1 and 2 only a single binding process is observed for FITC-PLL 319 ending at fluorescence intensity values of 0.3, 0.5 and 0.8.

The final values of normalized FITC-fluorescence intensity reveal to which extent PLL is binding to and penetrating the lipid membranes. A final value of 0.5 indicates that half of the amino acid residues are bound to lipid vesicles.

In Table 1 all final values for the normalized FITC-fluorescence intensity (at $R_P = 1$) after binding of the labeled peptides are given. In case of the short FITC-PLL 106 all normalized FITC-fluorescence intensity values lie in the range of 0.05 to 0.09 once binding is complete. The longer FITC-PLL 319, on the other hand, has final values between 0.46 and 0.63 for all membranes.

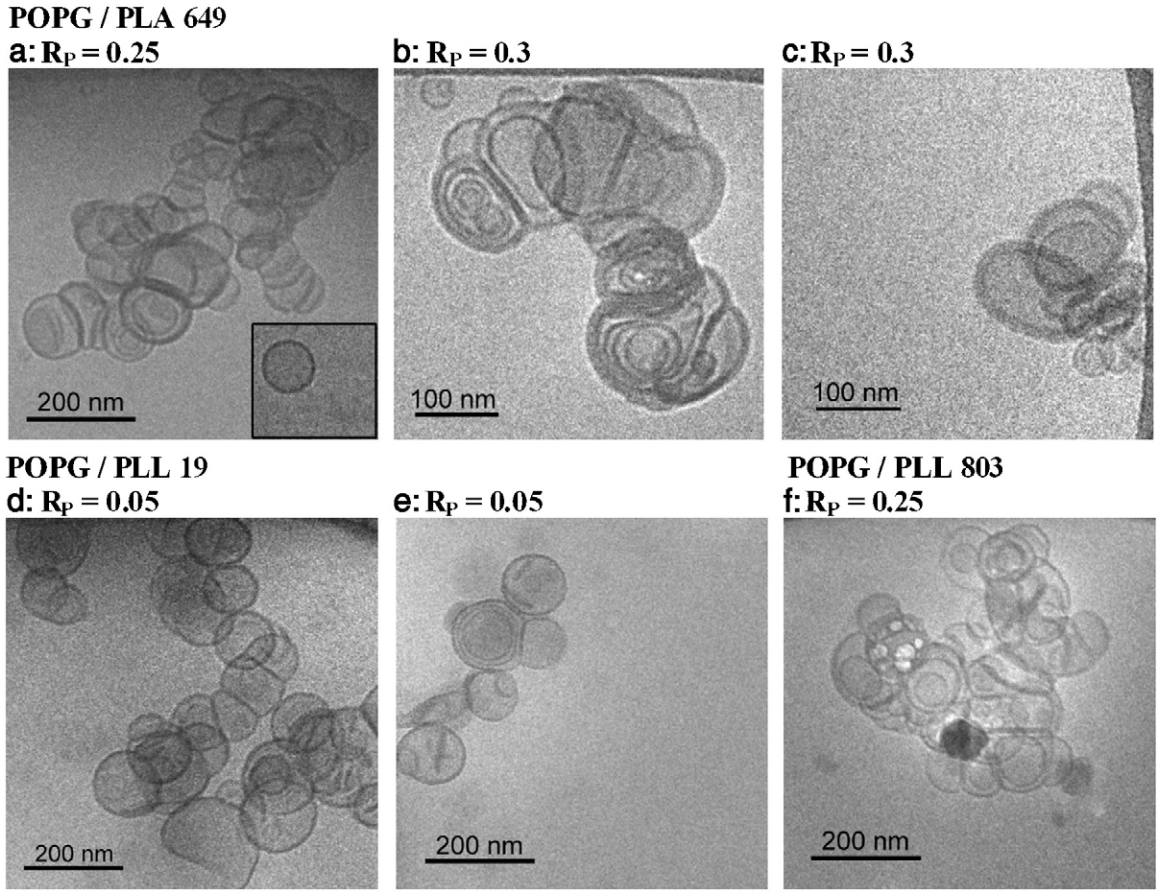

Fig. 5. Cryo-TEM images of PLA- and PLL-coated POPG vesicles. Cryo-TEM images of polypeptide-coated unilamellar POPG vesicles with PLA 649 at different R_P values (a–c), PLL 19 at $R_P = 0.05$ (d,e), and PLL 803 at $R_P = 0.25$ (f) prepared at 20 °C.

3.5. Binding of FITC-labeled PLA 69 and PLA 649

Binding of FITC-PLA 69 and FITC-PLA 649 to PG membranes leads to more diverse results. The shorter FITC-PLA 69 reaches for fluid membranes of POPG and POPG/POPC fluorescence intensity values of 0.26 and 0.21, respectively. In the case of the gel phase membranes of DPPG and DPPG/DPPC fluorescence intensity values of 0.1 and 0.12 are reached, respectively.

When FITC-PLA 649 binds to the fluid POPG membrane, a final value for the normalized fluorescence intensity of 0.17 is reached which is surprising as one would expect for the longer PLA that less side chains are bound to the membrane compared to its shorter homologue FITC-PLA 69, because of sterical reasons. In the case of the gel state DPPG- and both the fluid and gel phase PG/PC membranes, final fluorescence intensity values between 0.34 and 0.39 are reached, which are very similar compared to the values for the shorter PLA.

3.6. Cryo-TEM

As revealed by the dynamic light scattering and EM measurements (see inset of Fig. 5), the extruded suspension of 5 mM POPG without added polypeptide contains a homogeneous population of vesicles with an average diameter of 100–120 nm. No multilamellar structures were observed before polypeptide addition. The addition of the polypeptides PLA and PLL induced drastic changes in the vesicles' morphology. The formation of POPG-polypeptide aggregates is shown in Fig. 5 for PLA649, PLL19 and PLL803 for all investigated POPG-polypeptide ratios. In the case of PLA649 the aggregates are composed of several flattened vesicles that stick to each other (Fig. 5a–c). Some of these vesicles are no longer unilamellar but multilamellar. The thickness of the unilamellar PLA-coated vesicles reaches values of up to 15 nm. The PLL-coated vesicles also formed clusters of 10 to 100 vesicles. The vesicles were also deformed or flattened in the contact region (Fig. 5).

3.7. Isothermal titration calorimetry (ITC)

ITC experiments were performed to study the thermodynamics of PLL and PLA binding to lipid membranes, but generic differences to the fluorescence assays in the experimental parameters have to be taken into account. The first difference is that for ITC measurements higher lipid and peptide concentrations are needed to obtain a sufficient signal to noise ratio. Results of preliminary experiments (not shown) by fluorescence spectroscopy showed that the dye-release rate is increased with increasing peptide and lipid concentrations. The second difference is that in ITC experiments a peptide solution of high concentration was injected into a lipid vesicle suspension, whereas in the fluorescence assays a well-defined amount of lipid vesicles was injected only once into a peptide solution. Furthermore, in ITC repeated addition of small amounts of peptide solution into a lipid suspension takes place.

The ITC experiments were carried out with DPPG and DPPG/DPPC membranes, either above or below the main transition temperature T_m of ca. 41 °C.

3.8. PLL 402 binding to DPPG and DPPG/DPPC

The binding of PLL 402 to DPPG membranes at 20 and 60 °C (Fig. 6a) reveals a characteristic difference in binding to either gel phase or fluid membranes, respectively. The curve at 20 °C shows endothermic binding enthalpies with a maximum at $R_P = 0.29$ and falls to very low enthalpy values after $R_P = 0.5$. At 60 °C binding enthalpies are exothermic until an R_P value of 0.8 is reached. Thereafter, the binding enthalpy rises to endothermic values with a maximum at $R_P = 1$ and then decreases at $R_P = 1.3$ to values below 0.1 kcal mol^{-1}.

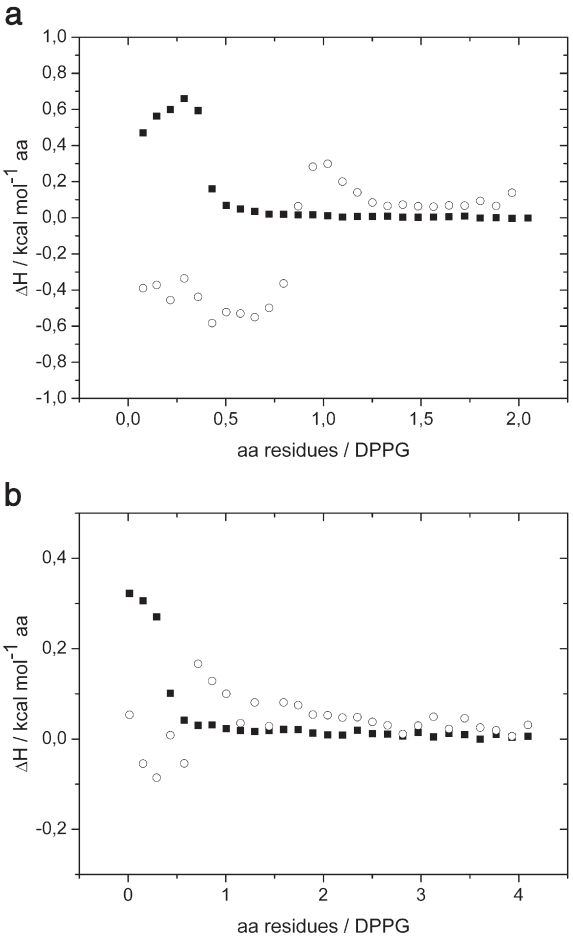

Fig. 6. ITC binding curves for PLL 402 to PG membranes. a): Reaction heats for the titration of 20 mM PLL 402 into a 2 mM DPPG suspension at 20 (■) and 60 (○) °C. b): Reaction heats for the titration of 20 mM PLL 402 into a 2 mM DPPG/DPPC (1/1 mol/mol) suspension at 20 (■) and 60 (○) °C.

The binding to a mixed DPPG/DPPC membrane should be similar, only that the electrostatic attraction to the membrane surface due to the dilution of the charges should be lower. The binding curves of PLL 402 to the mixed membranes DPPG/DPPC (Fig. 6b) at the same temperatures resemble in their shape indeed pretty much those for the pure DPPG membranes. Overall the binding enthalpies are smaller in the case of the mixed membranes and the data show more scatter for measurements at 60 °C.

3.9. PLL 803 binding to DPPG and DPPG/DPPC

Binding curves of the longer PLL 803 to DPPG and PG/PC membranes are shown in Fig. 7a–b. The curves for binding to the pure and the mixed membranes in the gel phase (at 20 °C) resemble each other very closely. The two curves are characterized by exothermic binding enthalpies for R_P smaller than 0.25. An increase of the binding enthalpies to ca. 0 kcal mol^{-1} (at $R_P = 0.29$) indicates the termination of PLL 803 binding to the gel phase membranes.

In the case of the pure fluid DPPG membrane at 60 °C PLL 803 binding occurs at least until an R_P value of 1. During the initial binding ($R_P = 0$ to 0.8) of PLL 803 binding enthalpies range mainly between −0.6 and −0.44 kcal mol^{-1}. In the final stages of this initial binding the binding enthalpy values become larger (ca. −1 kcal mol^{-1}) but are quite scattered. In the second part of the curve the binding enthalpy rises to endothermic values and then falls to 0.1 kcal mol^{-1} (at $R_P = 1$). The titration curve of PLL 803 to fluid, mixed DPPG/DPPC

membranes shows only small heat effects. Either there is no binding or the binding enthalpy becomes very low.

3.10. PLA 649 binding to DPPG and DPPG/DPPC

In case of the pure gel phase DPPG membrane at 30 °C PLA 649 binding to the membrane is first endothermic with a binding enthalpy of up to 0.45 kcal mol^{-1}. The binding enthalpy changes sign and becomes exothermic. The binding curve shows a characteristic minimum at an R_P value of 0.5 indicating peptide binding mainly to the outer membrane leaflet. Between R_P values of 0.5 and 1 the binding enthalpy vanishes and becomes essentially zero at an R_P value of 1.

Binding of PLA 649 to DPPG membranes in the fluid phase at 50 and 60 °C occurs with constant exothermic enthalpies ΔH of −1.5 kcal mol^{-1} until an R_P of 1 is reached (Fig. 8a). Between an R_P of 1 and 1.25 ΔH becomes zero. These two isotherms indicate a complete binding of PLA to both inner and the outer leaflets of lipid membranes in the fluid phase L_α.

The binding curves of PLA 649 to the mixed DPPG/DPPC membranes (Fig. 8b) have more or less a sigmoid shape, as expected for weaker binding due to reduced surface charge density of the lipid vesicles. All binding enthalpies are exothermic. For the gel phase membrane (30 °C) the binding enthalpies are somewhat smaller and the heat signals disappear at a ratio R_P of ca. 0.5. This indicates that only outside binding can take place in the gel phase. The titration curves for the fluid DPPG/DPPC membranes show also exothermic heats of binding. Here, the R_P values are shifted to higher values indicating that now the PLA 649 can reach the inner monolayer of the vesicles. The binding enthalpy seems to become more endothermic with increasing temperature.

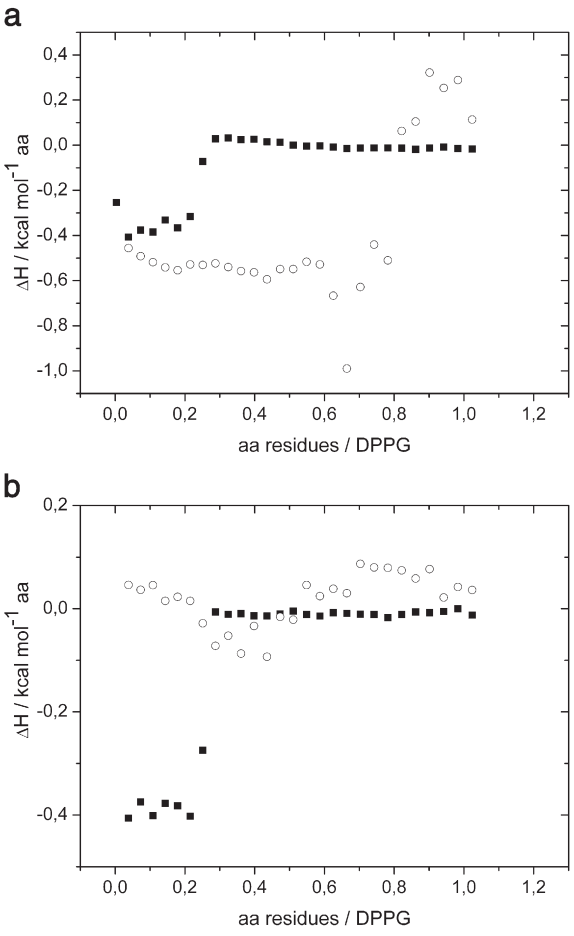

Fig. 7. ITC binding curves for PLL 803 to PG membranes. a): Reaction heats for the titration of 20 mM PLL 803 into a 2 mM DPPG suspension at 20 (■) and 60 (○) °C. b): Reaction heats for the titration of 20 mM PLL 803 into a 4 mM DPPG/DPPC (1/1 mol/mol) suspension at 20 (■) and 60 (○) °C.

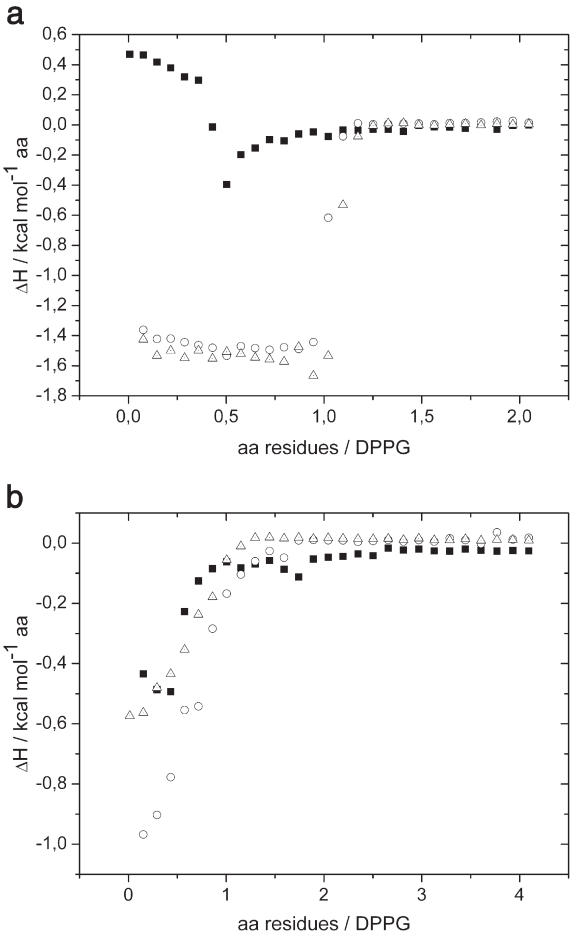

Fig. 8. ITC binding curves for PLA 649 to PG membranes. a): Reaction heats for the titration of 20 mM PLA 649 into a 2 mM DPPG suspension at 30 (■), 50 (○) and 60 (Δ) °C. b): Reaction heats for the titration of 20 mM PLA 649 into a 2 mM DPPG/DPPC (1/1 mol/mol) suspension at 30 (■), 50 (○) and 60 (Δ) °C.

4. Discussion

The positively charged polypeptides PLL and PLA adsorb to negatively charged phospholipid vesicles which leads to the formation of large aggregates around the isoelectric point [15,35]. In this paper we tried to analyze the processes that occur during peptide binding to lipid membranes and within the aggregate. In particular, leakage of an entrapped dye from lipid vesicles, translocation behavior of the charged polypeptides PLL and PLA and vesicle fusion were assayed using suitable fluorescence and microscopy methods, respectively. Isothermal titration calorimetry was applied to extend and confirm results obtained with the previous methods, in particular ITC was used to clarify whether the polypeptides can cross the membranes and bind to the inner monolayer of the vesicles.

4.1. Dye-release from phospholipid vesicles

Electrostatic interactions have a dominating influence in the adsorption of cationic polypeptides to phospholipid membranes [36]. Therefore, the molar ratio of amino acid residues to charged lipid molecules (PGs) R_P is an important quantity for the analysis of leakage and translocation processes. Besides pure electrostatic

interactions, hydrophobic and van-der-Waals interactions and hydrogen bonds can play a role in membrane binding processes. Lipid bilayers are composed of an outer and an inner leaflet where the latter one is not accessible for peptides during the initial binding event at low R_P values. However, during the binding to the membrane pores or defects may be formed which locally disrupt the barrier function so that an exchange of internal and external vesicle medium can take place. For most of the amphipathic peptides that have been extensively studied this exchange follows an all-or-none mechanism where a complete mixing of inner and outer medium occurs [37,11,38]. In the case of the less often observed graded mechanism [39] only a well-defined amount of dye solution is released from the vesicles. It is not known which mechanisms PLL and PLA follow. Experiments such as those presented by Heerklotz & Seelig [39] could not be performed, because the aggregates formed are too large to be purified by size-exclusion chromatography. Leakage from lipid vesicles can be due to both temporary pore formation, which is normally reversible, and complete vesicle lysis. If no leakage is observed, the vesicles are embedded in a peptide–lipid aggregate with non-disrupted (intact) membranes.

PLL induced dye-release from POPG and mixed PG/PC vesicles has been probed by several groups [16,2]. These groups either focused on a long-term kinetic investigation (over several days) and/or used completely different experimental conditions. In our paper a kinetic description of vesicle leakage on a short time scale is given for both PLLs and PLAs of different polymer lengths yielding a quantitative evaluation of membrane stability. Still, a reasonable number of interactions between phospholipid membranes and peptides, such as leakage, peptide adsorption, insertion and translocation and secondary structure changes, make the whole kinetic process very complex and do not allow to resolve the different influences on vesicle leakage from each other. Therefore, the analysis is limited to a qualitative level of understanding.

POPG membranes in the fluid L_α phase have a maximal leakage rate upon peptide binding that enables a proper observation of the induced processes (Fig. 1a and c for PLL 44 and PLA 69, resp.). At very low peptide concentrations ($R_P = 0.1$), both PLL and PLA adsorb to the membranes without an induction of pore formation. At an elevated peptide concentration ($R_P = 0.2$ to 0.4) kinetic curves have either an exponential shape in the case of PLL 44 indicating that only a single process contributes to the leakage or a bi-exponential shape revealing two processes that induce dye-release in the case of PLL 69. For R_P values between 0.4 and 0.7 kinetic curves for PLL 44 adopt a sigmoidal shape which suggests that leakage is decelerated when peptide binding starts, presumably due to hindered binding on the membrane surface at peptide excess. In the case of PLA 69 the bi-exponential leakage mechanism persists manifesting the superior binding capability of arginines over lysines [40].

At an R_P around 0.5 dye-release from POPG vesicles is maximal for all longer PLLs and PLAs (≥ 44), only PLL 19 shows an increasing dye-release until $R_P = 4$. Theoretically, at an $R_P = 0.5$ the outer monolayers are entirely covered with peptide molecules leading also to a maximal cross linking of vesicles. This cross linking of vesicles could be visualized for POPG vesicles covered with PLA 649. The POPG vesicles are deformed at the regions of contact with adjacent vesicles, but do not rupture. This strong deformation of the polypeptide-coated unilamellar vesicles indicates that the POPG-polypeptide interaction is either very strong or very asymmetric, or that the vesicles are very flexible [41].

When there is an excess of peptide molecules no leakage is observed because vesicles are fully covered with peptide that has a protection function on the surface [15]. Final values for the dye-release after finished kinetics provide a measure for the extent of pore formation and vesicle lysis which cannot be distinguished from each other. Thus, the term “membrane defects” is used to describe the present results.

PLAs induce more membrane defects than PLLs with a maximum of 70% for PLA 649 and 60% for PLL 44 (for POPG), respectively. A possible explanation for this finding is that the amino acid arginine with a protonated side chain can act as a hydrogen bond donor with five possible H-bonds to H-bond acceptors (like the ones present in the lipid head groups) whereas the protonated side chain of lysine can only form three which makes PLA a stronger binding partner [42]. Both for PLL and PLA the occurrence of membrane defects is decreased in the gel phase L_β (DPPG vesicles) proving that these membranes are more stable against peptide adsorption because of a less dynamic structure. For PLL 44 and 402 and PLA 184 there is a maximum in leakage from DPPG vesicles compared to both shorter and longer polymers. This finding can be explained on the basis of two counteracting effects: With increasing polymer length, the binding constant K_D is increased leading to a raised leakage rate. However, sterical effects gain weight with increasing polymer length that produce a decrease in dye-release. In the case of the mixed PG/PC membranes leakage is decreased to 30% in the case of the fluid membranes and it drops to less than 10% in the case of the gel phase membranes. Mainly, PCs are assumed to stabilize the membranes [22], while also reducing the membrane charge which explains the drop in leakage due to less close peptide binding on the membrane [30]. The mixed membranes have a maximal dye-release observed at R_P values of 1.3 (PLL 44 und PLA 69, data not shown). As a matter of fact, the reduced membrane charge requires more cationic polypeptide to reach substantial cross linking which is the prerequisite for membrane leakage.

Isothermal titration calorimetry confirmed that membranes in the fluid phase (DPPG at 60 °C) are more sensitive to leakage than gel phase membranes (DPPG at 20 °C) upon PLL (402 and 803) and PLA (649) binding (Figs. 6a–8a). In the fluid phase binding detected by enthalpy processes occurs until an $R_P \sim 1$ is reached which indicates that both inner and outer membrane leaflets are accessible to the cationic polypeptides, whereas in the gel phase peptide binding nearly stops when an $R_P \sim 0.5$ is reached.

For PLA 649 ITC also shows the strong difference in peptide binding to either DPPG or DPPG/DPPC membranes in the fluid phase. In the latter case the binding constant is much smaller, as a result of the decreased slope of binding enthalpy values. Peptide binding is also complete at an R_P of 1 revealing that the inner membrane leaflet is accessible for peptide binding, but not as a result of total vesicle lysis or pore formation which would have been detected by leakage. The ITC binding curve of PLA 649 and DPPG/DPPC in the gel phase (at 30 °C) which resembles the curve in the fluid phase is not suitable to explain the low dye-release, leaving open the possibility of membrane binding via alternative ways as for example peptide translocation into the inner membrane leaflet.

4.2. Peptide translocation through phospholipid membranes

FITC that is covalently bound to the PLL and PLA molecules serves as an ideal probe for peptide adsorption to phospholipid membranes and, furthermore, allows the evaluation of translocation properties of these peptides. The quantum yield of FITC strongly depends on the chemical environment which was examined by taking FITC spectra in different solvents. Roughly the quantum yield of FITC decreases several orders of magnitude with decreasing dielectric constant. As PLL or PLA is adsorbed to a phospholipid membrane FITC is intercalated between lipid molecules with their hydrophobic tails. FITC integrated into the membrane is then in an apolar environment and its normalized fluorescence intensity should drop to 0.5%. In the case of small R_P values (0.1 to 0.4) the normalized fluorescence intensity for the FITC-PLLs falls only to 5% which is probably due to the fact that not every FITC probe will be intercalated into the outer membrane leaflet. Another reason might be that FITC does not penetrate the membrane deep enough, i.e. is located in an

environment with slightly higher dielectric constant. The reason why the fluorescence intensity values of FITC-labeled PLAs drop only to values of 0.2 when binding to an excess of fluid (!) membranes is not fully clear but is also probably due to the location of the probe in the interface. We assume, however that at an R_P of 0.1 PLA is completely bound to the membrane.

The ability of PLL and PLA to penetrate and translocate through a lipid membrane was assayed depending on the state of the membrane, i.e. fluid or gel phase, and for both a short and a long polymer. Table 1 shows all obtained normalized fluorescence intensity values at an R_P of 1 after an incubation time of 840 s where both the processes of adsorption and translocation have finished. This R_P value was chosen because equal amounts of amino acid residues and lipids are present and enabled us to investigate to which extent PLL and PLA are bound to the inner and outer leaflets of the whole membrane. From the leakage experiments it was known that membranes suffer from PLL and PLA induced defects particularly in the fluid phase, but resist temporary pore formation better in the gel phase. PG/PC membranes exhibited even less membrane defects upon cationic polypeptide binding. A striking feature of the short FITC-PLL 106 upon binding to all examined membrane types is that always normalized fluorescence intensity values of less than 0.1 were observed which is in the same region as for the smallest investigated R_P value (0.1). Contrary to FITC-PLL 106, FITC-PLL 319 ends up at normalized fluorescence intensity values around 0.5 when probed with the four membrane types. These results suggest that the short FITC-PLL 106 is able to translocate through both fluid and gel phase membranes whereas the longer FITC-PLL 319 is not. Similar findings were reported earlier by Shibata et al. [20] who probed the translocation ability of FITC-PLL 106 (from the same supplier) through soybean phospholipid membranes with confocal microscopy.

The translocation ability of (oligo)peptides with high arginine content was described by several groups [14,13,43]. The short FITC-PLA 69 shows overall the same effect as the short FITC-PLL 106, so short PLA molecules translocate through lipid bilayers in a similar manner independent of membrane phase and composition. FITC-PLA 649 is two times longer than the investigated PLL counterpart, but seems to translocate through the fluid POPG membrane which is remarkable for a polymer of this length. At the same time one has to be aware that PLA 649 also induces a high leakage from phospholipid vesicles which may eventually result in lysis that would also make the inner leaflet easily accessible for peptide binding. An unambiguous interpretation of FITC-PLA 649 penetration through the fluid POPG bilayer is therefore not possible. Considering the low leakage rate of DPPG/DPPC membranes upon the binding of this peptide (8%) and a final value of the normalized fluorescence intensity of 0.39 suggests that at least 7% of the peptide molecules translocate (percentage of accessible inner lipid molecules = total value − inaccessible value measured in the assay − leakage rate/2 = 50% − 39% − (8%/2)) on the basis of total vesicle lysis and assuming an all-or-none mechanism. For both POPG/POPC and DPPG vesicles such an estimate is more difficult because there are maximal leakage rates of 30% which would mean that there is no translocation observed if vesicles that leak are totally lysed. 34% (DPPG) and 39% (POPG/POPC) of the initial fluorescence intensity remain at the end of peptide binding and translocation. ITC measurements confirm that there is a complete binding of PLA 649 to both inner and outer leaflets (until $R_P = 1$) of a DPPG membrane at 50 and 60 °C. As there is no total dye-release (only 70%) it can be confirmed that PLA 649 translocates through a fluid phospholipid membrane. The results for the gel phase and the mixed PG/PC membranes indicate that there is a decreased binding of PLA 649 to these membranes. However, heats of binding can be at least detected until an R_P of 1 is reached. Again, the problem that we cannot fully distinguish between possible but not known vesicle lysis and translocation does not permit a clear interpretation.

The ITC curves for PLL 402 which serves as a good equivalent to FITC-PLL 319 indicate a complete binding to both the inner and outer leaflets of the fluid phospholipid membrane (DPPG at 60 °C). This process was not observed in the FITC-assay raising the question for the reason for this difference. As mentioned above the concentration is much higher in the ITC experiment. This can enhance dye-release from phospholipid vesicles, particularly in the fluid phase (data not shown), and possibly can lead to increased peptide translocation ability through phospholipid membranes. Binding of PLL 402 to gel phase and mixed PG/PC membranes, however, confirms unambiguously that peptide binding takes place only on the outer membrane leaflet.

5. Conclusions

We have shown using fluorescence spectroscopy, isothermal titration calorimetry, and electron microscopy that the binding of poly-L-lysines and poly-L-arginines to negatively charged lipid vesicles is a process occurring in several steps which, depending on the charge ratio of lipid charges to amino acid side chain charges, can lead to the formation of membrane defects and to disruption of the vesicles and/or translocation of the polypeptides to the vesicle interior. The behavior of the system also depends on the total concentration of the binding partners and on the experimental procedures, i.e. whether the polypeptides are added to the lipid vesicles or *vice versa*. Fluid lipid vesicles are more easily penetrated by the polypeptides than gel state vesicles and comparing PLL and PLA the latter can more easily translocate through the membrane. The results show that only the combination of different techniques can shed light onto the binding and translocation process of cationic polypeptides.

References

[1] H.K. Kimelberg, D. Papahadjopoulos, Interaction of basic proteins with phospholipid membranes. Binding and changes in the sodium permeability of phosphatidylserine vesicles, J. Biol. Chem. 246 (1971) 1142.
[2] A.E. Gad, B.L. Silver, G.D. Eytan, Polycation-induced fusion of negatively-charged vesicles, Biochim. Biophys. Acta 690 (1982) 124.
[3] K. Fukushima, T. Noguchi, R. Shimozawa, Conformations of poly(L-lysine) induced by dimyristoylphosphatidylglycerol vesicles in alkaline buffer solutions, Fukuoka Daigaku Rigaku Shuho 22 (1992) 167.
[4] N. Sakai, S. Matile, Anion-mediated transfer of poly-L-arginine across liquid and bilayer membranes, J. Am. Chem. Soc. 125 (2003) 14348.
[5] B. Alberts, A. Johnson, J. Lewis, M. Raff, K. Roberts, P. Walter, Molecular Biology Of The Cell, Garland Science, New York, 2008.
[6] D. Lochmann, E. Jauk, A. Zimmer, Drug delivery of oligonucleotides by peptides, Eur. J. Pharm. Biopharm. 58 (2004) 237.
[7] T.P. Johnston, K.R. Kuchimanchi, H. Alur, M. Chittchang, A.K. Mitra, Inducing a change in the pharmacokinetics and biodistribution of poly-L-lysine in rats by complexation with heparin, J. Pharm. Pharmacol. 55 (2003) 1083.
[8] L. Arnold, A. Dagan, J. Gutheil, N. Kaplan, Antineoplastic activity of poly(L-lysine) with some ascites tumor cells, Proc. Natl. Acad. Sci. U.S.A. 76 (1979) 3246.
[9] K. Matsuzaki, O. Murase, K. Miyajima, Kinetics of pore formation by an antimicrobial peptide, magainin 2, in phospholipid bilayers, Biochemistry 34 (1995) 12553.
[10] A. Pokorny, T.H. Birkbeck, P.F. Almeida, Mechanism and kinetics of δ-lysin interaction with phospholipid vesicles, Biochemistry 41 (2002) 11044.
[11] J.L. Nieva, S. Nir, A. Muga, F.M. Goni, J. Wilschut, Interaction of the HIV-1 fusion peptide with phospholipid vesicles: different structural requirements for fusion and leakage, Biochemistry 33 (1994) 3201.
[12] A.D. Frankel, C.O. Pabo, Cellular uptake of the tat protein from human immunodeficiency virus, Cell 55 (1988) 1189.
[13] S.M. Fuchs, R.T. Raines, Pathway for polyarginine entry into mammalian cells, Biochemistry 43 (2004) 2438.
[14] E. Goncalves, E. Kitas, J. Seelig, Binding of oligoarginine to membrane lipids and heparan sulfate: structural and thermodynamic characterization of a cell-penetrating peptide, Biochemistry 44 (2005) 2692.
[15] D. Volodkin, V. Ball, P. Schaaf, J.-C. Voegel, H. Mohwald, Complexation of phosphocholine liposomes with polylysine. Stabilization by surface coverage versus aggregation, Biochim. Biophys. Acta 1768 (2007) 280.
[16] D. Volodkin, H. Mohwald, J.-C. Voegel, V. Ball, Coating of negatively charged liposomes by polylysine: drug release study, J. Control. Release 117 (2007) 111.
[17] D.H. Young, H. Kauss, Release of calcium from suspension-cultured glycine max cells by chitosan, other polycations, and polyamines in relation to effects on membrane permeability, Plant Physiol. 73 (1983) 698.

[18] S.M. Fuchs, R.T. Raines, Internalization of cationic peptides: the road less (or more?) traveled, Cell. Mol. Life Sci. 63 (2006) 1819.
[19] H.E. Davis, M. Rosinski, J.R. Morgan, M.L. Yarmush, Charged polymers modulate retrovirus transduction via membrane charge neutralization and virus aggregation, Biophys. J. 86 (2004) 1234.
[20] A. Shibata, S. Murata, S. Ueno, S. Liu, S. Futaki, Y. Baba, Synthetic copoly(Lys/Phe) and poly(Lys) translocate through lipid bilayer membranes, Biochim. Biophys. Acta 1616 (2003) 147.
[21] J. Bondeson, R. Sundler, Promotion of acid-induced fusion by basic peptides. Amino acid and phospholipid specificities, Biochim. Biophys. Acta 1026 (1990) 186.
[22] A. Walter, C.J. Steer, R. Blumenthal, Polylysine induces pH-dependent fusion of acidic phospholipid vesicles: a model for polycation-induced fusion, Biochim. Biophys. Acta 861 (1986) 319.
[23] K. Arnold, Handbook of biological physics, Vol. 1: structure and dynamics of membranes, in: R. Lipowsky, E. Sackmann (Eds.), Cation-Induced Vesicle Fusion Modulated by Polymers and Proteins, Chapter 19, Elsevier, 1995, p. 903.
[24] G. Förster, C. Schwieger, F. Faber, T. Weber, A. Blume, Influence of poly(L-lysine) on the structure of dipalmitoylphosphatidylglycerol/water dispersions studied by X-ray scattering, Eur. Biophys. J. 36 (2007) 425.
[25] C. Schwieger, A. Blume, Interaction of poly(L-lysines) with negatively charged membranes: an FT-IR and DSC study, Eur. Biophys. J. 36 (2007) 437.
[26] J. Seelig, Titration calorimetry of lipid–peptide interactions, Biochim. Biophys. Acta 1331 (1997) 103.
[27] K. Kawakami, Y. Nishihara, K. Hirano, Effect of hydrophilic polymers on physical stability of liposome dispersions, J. Phys. Chem. B 105 (2001) 2374.
[28] I. Tsogas, D. Tsiourvas, G. Nounesis, C.M. Paleos, Interaction of poly-L-arginine with dihexadecyl phosphate/phosphatidylcholine liposomes, Langmuir 21 (2005) 5997.
[29] K. Wagner, D. Harries, S. May, V. Kahl, J.O. Rädler, A. Ben-Shaul, Direct evidence for counterion release upon cationic lipid-DNA condensation, Langmuir 16 (2000) 303.
[30] C. Russ, T. Heimburg, H. von Grünberg, The Effect of lipid demixing on the electrostatic interaction of planar membranes across a salt solution, Biophys. J. 84 (2003) 3730.
[31] L. Fülöp, B. Penke, M. Zarandi, Synthesis and fluorescent labelling of beta-amyloid peptides, J. Pept. Sci. 7 (2001) 397.
[32] R.R.C. New, liposomes a practical approach (IRL Press at Oxford University Press Oxford–New York–Tokyo, 1990).
[33] P.S. Chen, T.Y. Toribara, H. Warner, Microdetermination of phosphorus, Anal. Chem. 28 (1956) 1756.
[34] C.H. Fiske, Y. Subbarow, The colorimetric determination of phosphorus, J. Biol. Chem. 66 (1925) 375.
[35] M. Reuter, Diploma thesis, Martin-Luther-University Halle-Wittenberg, Germany (2006).
[36] A.H. Juffer, C.M. Shepherd, H.J. Vogel, Protein membrane electrostatic interactions: application of the Lekner summation technique, J. Phys. Chem. 114 (2001) 1892.
[37] R. Blumenthal, P.J. Millard, M.P. Henkart, C.W. Reynolds, P.A. Henkart, Liposomes as targets for granule cytolysin from cytotoxic large granular lymphocyte tumors, Proc. Natl. Acad. Sci. U.S.A. 81 (1984) 5551.
[38] J.E. Cummings, D.P. Satchell, Y. Shirafuji, A.J. Ouellette, T.K. Vanderlick, Electrostatically controlled interactions of mouse paneth cell α-defensins with phospholipid membranes, Aust. J. Chem. 56 (2003) 1031.
[39] H. Heerklotz, J. Seelig, Leakage and lysis of lipid membranes induced by the lipopeptide surfactin, Eur. Biophys. J. 36 (2007) 305.
[40] D.J. Mitchell, D.T. Kim, L. Steinman, C.G. Fathman, J.B. Rothbard, Polyarginine enters cells more efficiently than other polycationic homopolymers, J. Peptide Res. 56 (2000) 318.
[41] S. Huebner, B.J. Battersby, R. Grimm, G. Cevc, Lipid-DNA complex formation: reorganization and rupture of lipid vesicles in the presence of DNA as observed by cryoelectron microscopy, Biophys. J. 76 (1999) 3158.
[42] M.G. Hutchings, M.C. Grossel, D.A.S. Merckel, A.M. Chippendale, M. Kenworthy, G. McGeorge, The structure of *m*-xylylenediguanidinium sulfate: a putative molecular tweezer ligand for anion chelation, Cryst. Growth Des. 1 (2001) 339.
[43] S. Futaki, T. Suzuki, W. Ohashi, T. Yagami, S. Tanaka, K. Ueda, Y. Sugiura, Arginine-rich peptides: an abundant source of membrane-permeable peptides having potential as carriers for intracellular protein delivery, J. Biol. Chem. 276 (2001) 5836.